Nanoscale

Accepted Manuscript

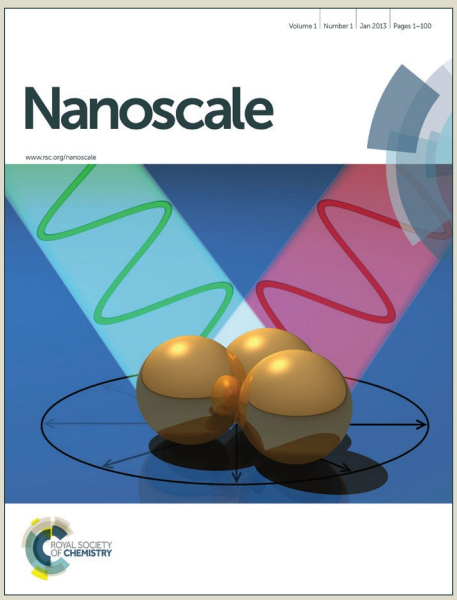

ROYAL SOCIETY OF CHEMISTRY

www.rsc.org/nanoscale

Nanoscale Paper

Supramolecular nanoreactors for intracellular singlet-oxygen sensitization†

Subramani Swaminathan,[a] Colin Fowley,[b] Ek Raj Thapaliya,[a] Bridgeen McCaughan,[b] Sicheng Tang,[a] Aurore Fraix,[c] Burjor Captain,[a] Salvatore Sortino,*[c] John F. Callan*[b] and Françisco M. Raymo*[a]

An amphiphilic polymer with multiple decyl and oligo(ethylene glycol) chains attached to a common poly(methacrylate) backbone assembles into nanoscaled particles in aqueous environments. Hydrophobic anthracene and borondipyrromethene (BODIPY) chromophores can be co-encapsulated within the self-assembling nanoparticles and transported across hydrophilic media. The reversible character of the noncovalent bonds, holding the supramolecular containers together, permits the exchange of their components with fast kinetics in aqueous solution. Incubation of cervical cancer (HeLA) cells with a mixture of two sets of nanoparticles, pre-loaded independently with anthracene or BODIPY chromophores, results in guest scrambling first and then transport of co-entrapped species to the intracellular space. Alternatively, incubation of cells with the two sets of nanocarriers in consecutive steps permits the sequential transport of the anthracene and BODIPY chromophores across the plasma membrane and only then allows their co-encapsulation within the same supramolecular containers. Both mechanisms position the two sets of chromophores with complementary spectral overlap in close proximity to enable the efficient transfer of energy intracellularly from the anthracene donors to the BODIPY acceptors. In the presence of iodine substituents on the BODIPY platform, intersystem crossing follows energy transfer. The resulting triplet state can transfer energy further to molecular oxygen with the concomitant production of singlet oxygen to induce cell mortality. Furthermore, the donor can be excited with two near-infrared photons simultaneously to permit the photoinduced generation of singlet oxygen intracellularly under illumination conditions compatible with applications *in vivo*. Thus, these supramolecular strategies to control the excitation dynamics of multichromophoric assemblies in the intracellular environment can evolve into valuable protocols for

[a] *Laboratory for Molecular Photonics, Department of Chemistry, University of Miami, 1301 Memorial Drive, Coral Gables, Florida, 33146-0431, United States. E-mail: fraymo@miami.edu*

[b] *School of Pharmacy and Pharmaceutical Sciences, University of Ulster, Coleraine, BT52 1SA, Northern Ireland, United Kingdom. E-mail: J.Callan@ulster.ac.uk*

[c] *Laboratory of Photochemistry, Department of Drug Sciences, University of Catania, Viale Andrea Doria 6, I-95125 Catania, Italy. E-mail: ssortino@unict.it*

† Electronic supplementary information (ESI) available: Experimental procedures; crystallographic data; absorption and emission spectra; temporal absorbance profiles; singlet-oxygen measurements; intracellular fluorescence measurements; viability assays. See DOI: 10.1039/#

photodynamic therapy.

Introduction

Noncovalent bonds guide the assembly of multiple molecular synthons into single supramolecular constructs.[1] The close proximity of the associated building blocks often impose electronic properties on the resulting assemblies that differ significantly from those of their individual components. In particular, the supramolecular association of distinct chromophores can have a pronounced influence on their excitation dynamics to allow the engineering of multicomponent assemblies with unique photochemical and photophysical properties.[2,3] Additionally, the inherent reversibility of noncovalent bonds imposes a dynamic character on supramolecular constructs.[4] Under appropriate experimental conditions, they can assemble and disassemble with relatively fast kinetics in solution. As a result, different supramolecular constructs can exchange their constituent components to enable the design of dynamic chemical ensembles that would be difficult, if at all possible, to replicate with the sole aid of covalent bonds.[5–9]

Amphiphilic polymers are valuable macromolecular synthons for the construction of supramolecular hosts capable of capturing a diversity of molecular guests in their interior.[10–16] Their covalent skeleton incorporates hydrophilic and hydrophobic segments that guide the assembly of multiple polymer chains into single particles of nanoscaled dimensions in aqueous environments. Solvophobic interactions bring the hydrophobic fragments of distinct polymer components in contact to minimize their direct exposure to water. Concomitant solvation of the hydrophilic fragments ensures optimal aqueous solubility and prevents further association of the nanoparticles into micro- and macro-scaled aggregates. The overall result is the spontaneous assembly of nanostructured constructs with hydrophilic surface and hydrophobic interior, where multiple hydrophobic guests can be encapsulated. In fact, such supramolecular hosts can transfer, otherwise insoluble, molecules into aqueous phases and carry them across hydrophilic media. Indeed, self-assembling nanoparticles of amphiphilic polymers are promising supramolecular vehicles for the transport of drugs across the blood stream in living organisms and their delivery to specific intracellular targets.[17–35]

In addition to guiding the assembly of multiple amphiphilic components into nanostructured particles, solvophobic interactions are also responsible for the ability of the resulting supramolecular hosts to encapsulate hydrophobic guests.[10–16] Once again, noncovalent contacts between the hydrophobic domains of the polymers and the entrapped molecules minimize the direct exposure of the latter species to the aqueous environment and maintain them inside the supramolecular containers. The very same interactions can be exploited to load hydrophobic guests with photoresponsive character in such nanostructured hosts.[36] The proximity of distinct chromophores within the interior of the nanoparticles can promote either electron or energy transfer to affect dramatically their excitation dynamics. In particular, the pairing of chromophores with overlapping emission and absorption bands within the same supramolecular container translates into the efficient transfer of excitation energy to permit the realization of luminescent materials with photophysical properties that cannot be reproduced with their separate components.[37–41] Furthermore, the occurrence of energy transfer between co-encapsulated guests is indicative of the integrity of their supramolecular hosts.[42–53] The disassembly of the nanocarriers into their constituent polymer components would otherwise separate donors from acceptors to prevent the transfer of energy from the former species to the latter. As a result, measurements of the donor and/or acceptor fluorescence can be employed to probe conveniently the stability of these nanocarriers and the possible leakage of their cargo into the surrounding aqueous environment. Similar measurements can also provide an indication of the dynamic character of the supramolecular hosts and their ability to exchange their guests.[42,44,45a,c,48,53] Specifically, the combination of nanoparticles, containing only donors, with nanocarriers, carrying exclusively acceptors, in the same solution can result in efficient energy transfer only if the two sets of supramolecular constructs can scramble their components to pair donors and acceptors within the same nanosized container.

We relied on the amphiphilic character of **1** (Fig. 1) to assemble hydrophilic supramolecular hosts for hydrophobic photochromic guests.[40,54] This particular polymer incorporates multiple decyl and oligo(ethylene glycol) chains along a common poly(methacrylate) backbone. In phosphate buffer saline (PBS), several copies of this macromolecule assemble into individual particles with an average

hydrodynamic diameter of 18 nm.[40] In the process of self-assembling, the nanoparticles can capture photochromic compounds in their hydrophobic interior to protect them from the surrounding aqueous environment and preserve their photochemical properties. In addition, such nanostructured hosts can transport their photoresponsive cargo across the membrane of living cells to permit the reversible switching of the photochromic guests, under optical control, within the intracellular space.[40,54d] Furthermore, distinct nanoparticles can exchange their components with fast kinetics, even after cellular internalization.[53] In fact, different guests can be transported inside the very same cell in consecutive steps to enable their interaction exclusively after internalization. For example, the sequential incubation of cells with two sets of nanoparticles of **1**, containing **2** and **3** (Fig. 1) respectively, results in the co-encapsulation of the two chromophoric guests in the same supramolecular container only in the intracellular space. The proximity enforced on them together with the optimal spectral overlap between the emission of **2** and the absorption of **3** translate into the efficient transfer of excitation energy from the former fluorophore to the latter. Under these conditions, significant acceptor emission is detected inside the incubated cells upon excitation of the donor. Thus, the dynamic character of the nanocarriers, responsible for transporting donors and acceptors independently across the cell membrane, ultimately allows their mutual interaction to enable the intracellular sensitization of fluorescence. On the basis of these results, we realized that such supramolecular strategy could be adapted to activate the sensitization of singlet oxygen, rather than fluorescence, in the intracellular space. Specifically, a chromophore capable of accepting the excitation energy of **2** to undergo efficient intersystem crossing could be employed, in place of **3**, to encourage the formation of singlet oxygen and induce significant cell mortality. In this article, we report the implementation of these innovative operating principles for the supramolecular activation of singlet-oxygen sensitizers inside living cells.

Results and discussion

Energy transfer between molecular guests entrapped within supramolecular hosts

Excitation of **2** produces significant fluorescence in the same spectral region where **3** absorbs.[53] The corresponding overlap integral is 9.1×10^{-14} M^{-1} cm^3. This value translates into a Förster distance of 47 Å that is comparable to the physical separation imposed on both chromophores with their co-encapsulation in nanoparticles of **1**. In fact, excitation of **2** at 430 nm, where the absorbance of **3** is negligible, results in the transfer of energy from the former guest to the latter with an efficiency of 95%. The co-entrapped energy acceptor has a fluorescence quantum yield of 0.51 and, once excited through the donor, emits intense fluorescence between 500 and 600 nm.

Literature data[55] indicate that the replacement of the ethyl groups of **3** with iodine substituents facilitates intersystem crossing with negligible influence on the absorption spectrum of the BODIPY chromophore. These observations suggest that the excitation energy of **2** can also be transferred to **4** (Fig. 1), if the two chromophores are co-entrapped in the same supramolecular container. Instead of decaying radiatively to the ground state, the excited acceptor can then intersystem cross to the corresponding triplet state and, in principle, transfer energy to molecular oxygen ($^3O_2$) and encourage the formation of singlet oxygen ($^1O_2$). On the basis of these considerations, we synthesized **4**, following a literature protocol,[55] and confirmed its structural identity by X-ray diffraction analysis (Fig. 1 and Table S1) of single crystals obtained from acetonitrile solution.

The absorption spectra (***a*** and ***b*** in Fig. 2) of **3** and **4** in tetrahydrofuran (THF) are remarkably similar. The replacement of the two ethyl groups with iodine substituents causes only a minor bathochromic shift and has essentially no influence on the molar absorption coefficient. Instead, the corresponding emission spectra (***c*** and ***d*** in Fig. 2) show a pronounced decrease in fluorescence intensity with iodine substitution. Specifically, the quantum yield drops from 0.72 to 0.03, in agreement with the expected ability of the two iodine atoms to promote intersystem crossing.

In analogy to **3**, **4** is also essentially insoluble in aqueous solutions, but readily dissolves in the presence of **1**. Furthermore, the encapsulation of **4** within the hydrophobic core of the resulting nanoparticles of **1** has no influence on the spectroscopic signature of the BODIPY chromophore. The absorption and emission bands, detected under these conditions, are identical to those recorded in THF

(Fig. S1). In particular, the main absorption of the entrapped guest (***c*** in Fig. 3) extends over the same spectral range as the emission of **2** (***b*** in Fig. 3), recorded under the same conditions. The corresponding overlap integral and Förster distance are 12.1×10^{-14} M^{-1} cm^3 and 49 Å respectively.[56] Both values are almost identical to those determined for **3**.[53] Thus, both BODIPY chromophores are expected to accept the excitation energy of the anthracene donor with similar efficiencies.

Mixing of **1**, **2** and **4** in chloroform, followed by evaporation of the solvent and treatment with PBS, results in the co-encapsulation of the two chromophores in nanoparticles of the polymer. The corresponding absorption spectrum (***d*** in Fig. 3) is essentially the sum of those (***a*** and ***c*** in Fig. 3) of the separate components entrapped in distinct nanocarriers. Examination of the individual spectra reveals that the absorbance of **2** at 430 nm is significant, while that of **4** at the same wavelength is negligible. In fact, excitation of the former compound at this wavelength produces intense fluorescence (***b*** in Fig. 3), while illumination of the latter results in minimal emission (***f*** in Fig. 3). When the two chromophores are encapsulated in the same nanocarrier, however, the emission intensity of the anthracene donor decreases and that of the BODIPY acceptor increases (***g*** in Fig. 3), demonstrating that the excitation energy of **2** is transferred to **4**. Specifically, the pronounced drop in donor emission (*cf.* ***b*** and ***g*** in Fig. 3) indicates the efficiency of energy transfer to be 93%.

These experiments prove that **4** is capable of accepting the excitation energy of **2**, when both species and **1** are treated together with PBS. Under these conditions, the self-assembling nanoparticles capture mixtures of donors and acceptors in their interior. A similar result is obtained also if donor and acceptor are entrapped individually in separate nanoparticles and then the two sets of nanocarriers are mixed in the same solution. In fact, the corresponding emission spectrum (***h*** in Fig. 3) shows again a dramatic decrease in the emission of the donor, relative to that of nanocarriers containing only **2** (***b*** in Fig. 3). Furthermore, normalization (***e*** in Fig. 3) of the latter spectrum to the former clearly reveals also an increase in acceptor fluorescence. Thus, the dynamic supramolecular hosts exchange their components with fast kinetics to co-localize donors and acceptors in the same nanostructured containers.

Singlet-oxygen sensitization within supramolecular containers

The two iodine substituents of **4** are responsible for the low fluorescence quantum yield because of their ability to promote intersystem crossing.[55] Consistently, the transient absorption spectrum (***a*** in Fig. 4), recorded 0.1 μs after pulsed-laser excitation at 355 nm, of nanoparticles of **1**, containing **4**, shows the characteristic triplet–triplet absorption of the BODIPY chromophore at *ca.* 420 nm and the bleaching of its ground-state absorption at *ca.* 530 nm. The absorbance at the former wavelength decays and that at the latter recovers with first-order kinetics and a lifetime of *ca.* 30 μs (Fig. S2). These spectral and kinetic outputs are fully consistent with literature data,[55] determined in degassed acetonitrile, and demonstrate that the lowest triplet state of **4** is populated upon excitation, even when this compound is entrapped within the supramolecular container. In the presence of **2**, the very same triplet–triplet absorption is also observed in the corresponding transient spectrum (***b*** in Fig. 4). Even although **2** absorbs most of the exciting photons, under these particular conditions, similar absorbance changes for the transient bands at 420 and 530 nm are detected. These results and the pronounced decrease in the fluorescence of **2**, observed when this species is co-encapsulated with **4** in the nanoparticles (*cf.* ***b*** and ***g*** in Fig. 3), indicate that the excitation energy of **2** is transferred to **4** with the subsequent population of its lowest triplet state.

In aerated solution, the lowest triplet state of **4** can transfer energy to $^3O_2$ with the concomitant formation of $^1O_2$. Consistently, the emission spectrum (***d*** in Fig. 4), recorded upon excitation at 405 nm, of nanoparticles of **1**, containing **4**, shows the characteristic phosphorescence of $^1O_2$ at 1270 nm.[57] Comparison of the integrated emission intensity to that detected for an optically-matched acetonitrile solution of **4**, under identical illumination conditions, indicates the quantum yield of $^1O_2$ to be 0.55.[58] The assignment of this emission band to the radiative relaxation of $^1O_2$ is further confirmed by the typical microsecond decay with first-order kinetics of the emission intensity at 1270 nm (***f*** in Fig. 4). In the presence of **2**, the phosphorescence (***e*** in Fig. 4) increases significantly, under otherwise identical conditions, indicating that the fraction of photons absorbed by the anthracene chromophores contributes to the formation of $^1O_2$.[59] However, no emission (***c*** in Fig. 4) can be detected if only **2** is

encapsulated within the supramolecular containers. These observations demonstrate that the presence of **4** is essential to mediate the transfer of the excitation energy of **2** to $^3O_2$ and promote the formation of $^1O_2$.

The ability of the supramolecular nanocarriers, co-encapsulating **2** and **4**, to sensitize $^1O_2$ is further confirmed by fluorescence measurements performed in the presence of singlet-oxygen sensor green (SOSG). This particular nonemissive compound reacts with $^1O_2$ to generate a fluorescent product.[60] In fact, the characteristic fluorescence of the product is observed after irradiation of a PBS solution of SOSG and the nanoparticles loaded with both **2** and **4** (Fig. S4). By contrast, negligible emission can only be detected if only one of the two guests is entrapped within the supramolecular host, under otherwise identical conditions.

Intracellular singlet-oxygen sensitization

Literature precedents[40,53,54d] demonstrate that nanoparticles of **1** can cross the membrane of living cells and transport their cargo to the intracellular space. Consistently, the incubation of HeLA cells with nanocarriers containing **2** results in significant intracellular fluorescence (*cf.* ***a*** and ***b*** in Fig. 5).[61] The images (***d*** and ***e*** in Fig. 5), recorded after incubation, clearly show that the fluorescent nanoparticles are distributed throughout the cytosol with negligible nuclear localization. In the presence of **4** within the same supramolecular containers, however, the excitation energy of the anthracene chromophores is transferred efficiently to the co-encapsulated BODIPY acceptors with the concomitant suppression of the donor emission. As a consequence, only negligible intracellular fluorescence (***c*** and ***f*** in Fig. 5) can be detected, after incubation of the cells with supramolecular hosts containing both guests under otherwise identical conditions.

The intracellular fluorescence measurements (***b*** and ***c*** in Fig. 5) are fully consistent with the spectroscopic data (***b*** and ***g*** in Fig. 3). In both instances, the co-encapsulation of **2** and **4** within nanoparticles of **1** ensures the transfer of energy from the anthracene donors to the BODIPY acceptors upon excitation. These observations suggest that the excitation dynamics of the co-entrapped guests

can be exploited to sensitize $^1O_2$ also in the intracellular space and induce cell mortality as a result. Control experiments on HeLA cells incubated with nanoparticles of **1**, containing increasing amounts of **2**, **4** or a mixture of both, indicate that the loaded nanocarriers have no cytotoxic effects, if the cells are maintained in the dark.[62] Specifically, the viability (● of ***a***–***c*** in Fig. 6), measured after storing the cells for 24 hours in the dark, is close to 100% in all instances. Essentially the same result (○ of ***a*** in Fig. 6) is obtained if the cells, containing nanoparticles loaded exclusively with **2**, are illuminated at 435 nm for 30 s with a continuous-wave laser prior to storage.[63] At this particular wavelength, the anthracene chromophores absorb significantly (***a*** in Fig. 3), but they are unable to sensitize $^1O_2$ on their own and, therefore, their excitation has no cytotoxic effects. Similarly, only a modest viability decrease (○ of ***b*** in Fig. 6) is detected after irradiation of cells incubated with nanoparticles containing exclusively **4**. The direct excitation of the BODIPY chromophores could promote the formation of $^1O_2$, but their molar absorption coefficient at 435 nm is negligible (***c*** in Fig. 3) and, hence, these particular illumination conditions have a minor influence on cell viability. When both guests are co-encapsulated in the same supramolecular hosts, however, the excitation energy of **2** can be transferred to **4** and promote the formation of a significant amount of $^1O_2$. Indeed, the viability (○ of ***c*** in Fig. 6) decreases drastically after the illumination of cells containing nanoparticles loaded with both guests.

The ability of the supramolecular nanocarriers to sensitize $^1O_2$ intracellularly is a consequence of their dynamic character. Indeed, the two sets of nanoparticles, pre-loaded independently with donors and acceptors, are mixed in the extracellular space to exchange of their components with fast kinetics and produce supramolecular containers with both chromophores in their interior. Then, the nanocarriers travel across the plasma membrane to transport their cargo inside the cells, where they mediate the photoinduced generation of $^1O_2$. Alternatively, the cells can be incubated sequentially with the two sets of nanoparticles to enable guest exchange in the intracellular space. Under these conditions, significant production of $^1O_2$ can occur inside the incubated cells only after the second internalization step. In fact, the viability of cells treated with nanoparticles of **1**, containing increasing amounts of **2**, first and then nanocarriers of **1**, containing equivalent amounts of **4**, clearly shows significant mortality with illumination (*cf.* ● and ○ of ***a*** in Fig. 7). Furthermore, the very same result (*cf.* ● and ○ of ***b*** in Fig.

7) is obtained if the order of the two incubation steps is reversed. In both instances, the recorded viabilities are essentially identical to those measured for cells incubated with both sets of nanoparticles simultaneously (*cf.* ○ of ***c*** in Fig. 6 and ○ of ***a*** and ***b*** in Fig. 7). Thus, these results demonstrate that the sequential transport of complementary chromophores in the intracellular space in conjunction with the ability of the nanocarriers to exchange their components can be exploited to activate sensitization and induce cell mortality.

The two-photon absorption cross sections of 9,10-bis(arylethynyl)anthracene derivatives are in excess of 100 GM at 900 nm.[64,65] This relatively large value, in conjunction with the excitation dynamics of **2** and **4** co-encapsulated within the same supramolecular hosts, offers the opportunity to sensitize $^1O_2$ effectively under the influence of near-infrared radiations.[66] Once again, control experiments show that nanoparticles of **1**, containing **2**, **4** or both, have no effects on the viability (● of ***a–d*** in Fig. 8) of cells maintained in the dark for 24 hours. Illumination of the cells at 900 nm with a pulsed laser prior to storage in the dark has no influence on the cells (○ of ***a*** in Fig. 8), even when they contain nanocarriers loaded with **2** (○ of ***b*** in Fig. 8). Even although the anthracene chromophores are excited at this particular wavelength, they cannot promote the formation of $^1O_2$ and have no influence on cell viability. Similarly, a modest decrease in viability (○ of ***c*** in Fig. 8) is detected when **4** is exclusively present in the nanocarriers, indicating that the direct excitation of the BODIPY chromophores is negligible under these illumination conditions. By contrast, the viability drops to only 30% (○ of ***d*** in Fig. 8) when both guests are within the same supramolecular containers. Indeed, the two-photon excitation of the anthracene donors can be followed by energy transfer to the BODIPY acceptors, intersystem crossing of the latter chromophores and sensitization of a significant amount of $^1O_2$ in the intracellular space. Thus, the unique combination of photophysical properties engineered into these supramolecular constructs ensures significant cell mortality under illumination conditions that are ideal for applications *in vivo*.

Conclusions

Self-assembling nanoparticles of amphiphilic polymers can capture anthracene donors and BODIPY acceptors within their hydrophobic interior and transport them across hydrophilic environments. The optimal spectral overlap between the emission of the donor and the absorption of the acceptor as well as their close proximity inside the nanostructured containers ensure the efficient transfer of excitation energy from one chromophore to the other. The introduction of two iodine substituents on the BODIPY platform does not alter its ability to accept the excitation energy of the anthracene partner. However, the two heavy atoms promote intersystem crossing and allow the population of the triplet state of the acceptor, after the excitation of the donor. In aerated solutions, energy can be further transferred to molecular oxygen to produce singlet oxygen. The suppression of the donor fluorescence, the appearance of the acceptor triplet–triplet absorption and the detection of singlet-oxygen phosphorescence are fully consistent with these excitation dynamics. Furthermore, the dynamic character of these supramolecular nanocarriers ensures the exchange of their components with fast kinetics in aqueous solution. Indeed, nanoparticles, loaded independently with donors and acceptors, barter their cargo upon mixing to co-encapsulate the complementary chromophores within the same supramolecular containers and enable energy transfer. The guest exchange between independent hosts can occur in the extracellular space, if cells are incubated with a mixture of the two sets of nanoparticles, or in the intracellular space, if they are incubated with the two types of nanocarriers in consecutive steps. In both instances, donors and acceptors are ultimately co-localized in close proximity within the cells and their ability to mediate singlet oxygen upon excitation induces significant cell mortality. Furthermore, the anthracene donor can be excited with two near-infrared photons simultaneously to enable the sensitization of singlet oxygen intracellularly under illumination conditions compatible with applications *in vivo*. Thus, our strategy for the sensitization of singlet oxygen inside cells might ultimately evolve into a viable protocol for photodynamic therapy under supramolecular control.

Acknowledgements

SS acknowledges support from AIRC (Project IG-12834) and MIUR (PRIN 2011). JFC acknowledges support from Norbrook Laboratories Ltd. FMR acknowledges support from NSF (CHE-1049860).

Notes and references

1 (a) J.-M. Lehn, *Proc. Natl. Acad. Sci. U.S.A.*, 2002, ***99***, 4763; (b) J.-M. Lehn, *Science*, 2002, ***295***, 2400.

2 V. Ramamurthy and Y. Inoue (Eds.), *Supramolecular Photochemistry, Controlling Photochemical Processes*, Wiley, New York, 2011.

3 A. Credi (Ed.), Themed Issue on "Supramolecular Photochemistry", *Chem. Soc. Rev.*, 2014, ***43***, 3995.

4 J. R. Nitschke (Ed.), Themed Issue on "Supramolecular and Dynamic Covalent Reactivity", *Chem. Soc. Rev.*, 2014, ***43***, 3995.

5 (a) J.-M. Lehn, Chem. *Eur. J.*, 1999, ***5***, 2455; (b) J.-M. Lehn, *Chem. Eur. J.*, 2000, ***12***, 2097; (c) J.-M. Lehn, *Chem. Soc. Rev.*, 2007, ***36***, 151; (d) J.-M. Lehn, *Top. Curr. Chem.*, 2012, ***322***, 1; (e) J.-M. Lehn, *Angew. Chem. Int. Ed.*, 2013, ***52***, 2836.

6 (a) S. J. Rowan, S. J. Cantrill, G. R. L. Cousins, J. K. M. Sanders and J. F. Stoddart, *Angew. Chem. Int. Ed.*, 2002, **41**, 899; (b) M. Belowich and J. F. Stoddart, *Chem. Soc. Rev.*, 2012, ***41***, 2003; (c) J. F. Stoddart, *Angew. Chem. Int. Ed.*, 2012, ***51***, 12902.

7 J. D. Cheeseman, A. D. Corbett, J. L. Gleason and R. J. Kazlauskas, *Chem. Eur. J.*, 2005, ***11***, 1708.

8 (a) P. T. Corbett, J. Leclaire, L. Vial, K. R. West, J.-L. Wietor, J. K. M. Sanders and S. Otto, *Chem. Rev.,* 2006, ***106***, 3652; (b) F. B. L. Cougnon and J. K. M. Sanders, *Acc. Chem. Res.,* 2012, ***45***, 2211.

9 S. Ladame, *Org. Biomol. Chem.*, 2008, ***6***, 219.

10 (a) A. Halperin, M. Tirrell and T. P. Lodge, *Adv. Polym. Sci.*, 1992, ***100***, 31; (b) T. P. Lodge, *Macromol. Chem. Phys.,* 2003, ***204***, 265; (c) A. O. Moughton, M. A. Hillmyer and T. P. Lodge, *Macromolecules*, 2012, ***45***, 2.

11 (a) M. Moffitt, K. Khougaz and A. Eisenberg, *Acc. Chem. Res.*, 1996, ***29***, 95; (b) N. S. Cameron, K. M. Corbierre, and A. Eisenberg, *Can. J. Chem*., 1999, ***77***, 1311.

12 S. E. Webber, *J. Phys. Chem. B*, 1998, ***102***, 2618.

13 G. Riess, *Prog. Polym. Sci.*, 2003, ***28***, 1107.

14 I. M. Okhapkin, E. E. Makhaeva and A. R. Khokhlov, *Adv. Polym. Sci.*, 2006, ***195***, 177.

15 T. S. Kale, A. Klaikherd, B. Popere and S. Thayumanavan, *Langmuir*, 2009, ***25***, 9660.

16 S. C. Owen, D. P. Y. Chan and M. S. Shoichet, *Nano Today*, 2012, *7*, 53.

17 H. Bader, H. Ringsdorf and B. Schmidt, *Angew. Makromol. Chem.*, 1984, ***123***, 457.

18 K. Kataoka, G. S. Kwon, M. Yokoyama, T. Okano and Y. Sakurai, *J. Control Release*, 1993, ***24***, 119.

19 M.-C. Jones and J.-C. Leroux, *Eur. J. Pharm. Biopharm.*, 1999, ***48***, 101.

20 V. P. Torchilin, *J. Control Release*, 2001, ***73***, 137.

21 M. L. Adams, A. Lavasanifar and G. S. Kwon, *J. Pharm. Sci.*, 2003, ***92***, 1343.

22 A. G. Husseini and W. G. Pitt, *Adv. Drug Deliv. Rev.*, 2008, ***60***, 1137.

23 K. Mondon, R. Gurny and M. Moller, *Chimia*, 2008, ***62***, 832.

24 J. H. Park, S. Lee, J. H. Kim, K. Park, K. Kim and I. C. Kwon, *Prog. Polym. Sci.*, 2008, ***33***, 113.

25 S. Kim, Y. Shi, J. Y. Kim, K. Park and J.-X. Cheng, *Expert Opin. Drug. Deliv.*, 2010, *7*, 49.

26 (a) R. T. Chacko, J. Ventura, J. Zhuang and S. Thayumanavan, *Adv. Drug. Deliv. Rev.*, 2012, ***64***, 836; (b) J. Zhuang, M. R. Gordon, J. Ventura, L. Li and S. Thayumanavan, *Chem. Soc. Rev.*, 2013, ***42***, 7421.

27 Y. Wang and S. M. Grayson, *Adv. Drug Deliv. Rev.*, 2012, ***64***, 852.

28 A. Lalatsa, A. G. Schatzlein, M. Mazza, B. H. L. Thi and I. F. Uchegbu, *J. Control. Rel.*, 2012, ***161***, 523.

29 (a) J. Nicolas, S. Mura, D. Brambilla, N. Mackiewicz and P. Couvreur, *Chem. Soc. Rev.,* 2013, ***42***, 1147; (b) S. Mura, J. Nicolas and P. Couvreur, *Nat. Mater.*, 2013, ***12***, 991.

30 Y. Lu and K. Park, *Int. J. Pharm.*, 2013, ***452***, 198.

31 J. Y. Tyler, X.-M. Xu and J.-X. Cheng, *Nanoscale*, 2013, ***5***, 8821.

32 D. R. Wang and X. G. Wang, *Prog. Polym. Sci.*, 2013, ***38***, 271.

33 L. Gu, A. Faig, D. Abdelhamid and K. Uhrich, Acc. *Chem. Res.*, 2014, ***47***, 2867.

34 D. Y. Alakhova and A. V. Kabanov, *Mol. Pharm.*, 2014, ***11*****,** 2566.

35 A. Makino, *Polym. J.*, 2014, ***46***, 783.

36 S. Swaminathan, J. Garcia-Amorós, A. Fraix, N. Kandoth, S. Sortino and F. M. Raymo, *Chem. Soc. Rev.*, 2014, ***43***, 4167.

37 (a) S. I. Yoo, S. J. An, G. H. Choi, K. S. Kim, G.-C. Yi, W.-C. Zin, J. C. Jung and B.-H. Sohn, *Adv. Mater.*, 2007, ***19***, 1594; *(*b) S. I. Yoo, J.-H. Lee, B.-H. Sohn, I. Eom, T. Joo, S. J. An and G.-C. Yi, *Adv. Funct. Mater.*, 2008, ***18***, 2984.

38 W.-C. Wu, C.-Y. Chen, Y. Tian, S.-H. Jang, Y. Hong, Y. Liu, R. Hu, B. Z. Tang, Y.-T. Lee, C.-T. Chen, W.-C. Chen and A. K.-Y. Jen, *Adv. Funct. Mater.*, 2010, ***29***, 1413.

39 R. Wang, J. Peng, F. Qiu and Y. Yang, *Chem. Commun.*, 2011, ***47***, 2787.

40 I. Yildiz, S. Impellizzeri, E. Deniz, B. McCaughan, J. F. Callan and F. M. Raymo, *J. Am. Chem. Soc.*, 2011, ***133***, 871.

41 A. Wagh, S. Y. Qian and B. Law, *Bioconjugate Chem.*, 2012, ***23***, 981.

42 Y. Hu, M. C. Kramer, C. J. Boudreaux and C. L. McCormick, *Macromolecules*, 1995, ***28***, 7100.

43 (a) H. Chen, S. Kim, W. He, H. Wang, P. S. Low, K. Park and J. X. Cheng, *Langmuir*, 2008, ***24***, 5213; (b) H. T. Chen, S. W. Kim, L. Li, S. Y. Wang, K. Park and J. X. Cheng, *Proc. Natl. Acad. Sci. USA*, 2008, ***105***, 6596; (c) S.-Y. Lee, J. Y. Tyler, S. Kim, K. Park and J.-X. Cheng, *Mol. Pharmaceutics*, 2013, ***10***, 3497.

44 G. N. Njikang, M. Gauthier and J. M. Li, *Polymer*, 2008, ***49***, 5474.

45 (a) S. Jiwpanich, J. H. Ryu, S. Bickerton and S. Thayumanavan, *J. Am. Chem. Soc.*, 2010, ***132***, 10683; (b) J. H. Ryu, R. T. Chacko, S. Jiwpanich, S. Bickerton, R. P. Babu and S. Thayumanavan, *J. Am. Chem. Soc.*, 2010, ***132***, 17227; (c) S. Bickerton, S. Jiwpanich and S. Thayumanavan, *Mol. Pharmaceutics*, 2012, ***9***, 3569.

46 K. J. Chen, Y. L. Chiu, Y. M. Chen, Y. C. Ho and H. W. Sung, *Biomaterials*, 2011, ***32***, 2586.

47 J. Lu, S. C. Owen and M. S. Shoichet, *Macromolecules*, 2011, ***44***, 6002.

48 P. Hua and N. Tirelli, *React. Funct. Polym.*, 2011, ***71***, 303.

49 T. O. McDonald, P. Martin, J. P. Patterson, D. Smith, M. Giardiello, M. Marcello, V. See, R. K. O'Reilly, A. Owen and S. Rannard, *Adv. Funct. Mater.*, 2012, ***22***, 2469.

50 (a) Y. P. Li, M. S. Budamagunta, J. T. Luo, W. W. Xiao, J. C. Voss and K. S. Lam, *ACS Nano*, 2012, ***6***, 9485; (b) Y. P. Li, W. W. Xiao, K. Xiao, L. Berti, J. T. Luo, H. P. Tseng, G. Fung and K. S. Lam, *Angew. Chem. Int. Ed.*, 2012, ***51***, 2864.

51 N. M. Javali, A. Raj, P. Saraf, X. Li and B. Jasti, *Pharm. Res.*, 2012, ***29***, 3347.

52 A. S. Klymchenko, E. Roger, N. Anton, H. Anton, I. Shulov, J. Vermot, Y. Mely and T. F. Vandamme, *RSC Advances*, 2012, ***2***, 11876.

53 S. Swaminathan, C. Fowley, B. McCaughan, J. Cusido, J. F. Callan and F. M. Raymo, *J. Am. Chem. Soc.*, 2014, ***136***, 7907.

54 (a) J. Cusido, M. Battal, E. Deniz, I. Yildiz, S. Sortino and F. M. Raymo, *Chem. Eur. J.*, 2012, ***18***, 10399; (b) E. Deniz, M. Tomasulo, J. Cusido, I. Yildiz, M. Petriella, M. L. Bossi, S. Sortino, and F. M. Raymo, *J. Phys. Chem. C*, 2012, ***116***, 6058; (c) S. Swaminathan, M. Petriella, E. Deniz, J. Cusido, J. D. Baker, M. L. Bossi and F. M. Raymo, *J. Phys. Chem. A*, 2012, ***116***, 9928; (d) M. Petriella, E. Deniz, S. Swaminathan, M. J. Roberti, F. M. Raymo and M. L. Bossi, *Photochem. Photobiol.*, 2013, ***89***, 1391.

55 W. Wu, H. Guo, W. Wu, S. Ji and J. Zhao, *J. Org. Chem.*, 2011, ***76***, 7056.

56 The overlap integral (J) and Förster distance (R_0) were calculated with equations (1) and (2) respectively (Lakowicz, J. R. *Principles of Fluorescence Spectroscopy*; Springer: New York, 2006). The emission intensity (I_D) of the anthracene donor and the molar absorption coefficient (ε_A) of the BODIPY acceptor at a given wavelength (λ) were determined from the corresponding emission and absorption spectra (***b*** and ***c*** in Fig. 3) respectively. The orientation factor (κ^2), fluorescence quantum yield (ϕ_D) of the donor and refractive index (n) of the solvent are 2/3, 0.61 and 1.328 respectively.

$$J = \frac{\int_0^\infty I_D \, \varepsilon_A \, \lambda^4 \, d\lambda}{\int_0^\infty I_D \, d\lambda} \qquad (1)$$

$$R_0 = \sqrt[6]{\frac{9000 \, (\ln 10) \, \kappa^2 \, \phi_D \, J}{128 \, \pi^5 N \, n^4}} \qquad (2)$$

57 F. Wilkinson, W. P. Helman and A. B. Ross, *J. Phys. Chem. Ref. Data*, 1993, ***22***, 113.

58 The quantum yield (Φ_Δ) of $^1O_2$ for nanoparticles of **1**, containing **4**, dissolved in D_2O was determined against an optically-matched solution of **4** in MeCN with eq. (3) (A. P. Darmanyan, *J. Phys. Chem. A* 1998, **102**, 9833). The quantum yield ($\Phi_{\Delta(S)}$) of $^1O_2$ for the standard is 0.79 (Huang, L.; Zhao, J.; Guo, S.; Zhang, C.; Ma, J. *J. Org. Chem.* 2013, **78**, 5626). The integrated emission intensities of nanoparticles (I) and standard ($I_{(S)}$) were estimated from the corresponding spectra (***d*** in Fig. 4). The refractive indexes of D_2O (n) and MeCN ($n_{(S)}$) are 1.328 and 1.335 respectively. The rate constants for the radiative decay of $^1O_2$ in D_2O (k_r) and MeCN ($k_{r(S)}$) are 0.18 and 0.45 s^{-1} respectively.

$$\Phi_\Delta = \frac{\Phi_{\Delta(S)} \, I \, n^2 \, k_{r(S)}}{I_{(S)} \, n_{(S)}^2 \, k_r} \qquad (3)$$

59 In degassed solution, the band at 1270 nm cannot be detected in agreement with its assignment to $^1O_2$ (Fig. S3).

60 C. Flors, M. J. Fryer, J. Waring, B. Reeder, U. Bechtold, P. M. Mullineaux, S. Nonell, M. T. Wilson and N. R. Baker, *J. Exp. Bot.*, 2006, ***57***, 1725.

61 The temporal evolution of the intracellular fluorescence (Fig. S5) suggests that the incubation of cells and nanoparticles for up to 3 hours translates into the internalization of relatively large amounts of fluorescent nanocarriers. As a result, all cellular uptake experiments were performed with this particular incubation time.

62 Viability assays (Fig. S6) on human umbilical vein endothelial cells (HUVECs) and human skin fibroblasts (Hs 27) demonstrate that nanoparticles of **1**, containing either **2** or **4**, do not have any cytotoxic effects in the dark also on normal cells.

63 These particular illumination conditions ensure the delivery of the highest possible light dose with negligible cytotoxicity in the absence of the nanoparticles. They were selected after testing the influence of the irradiation time on cell viability (Fig. S7).

64 W. J. Yang, C. H. Kim, M.-Y. Jeong, S. K. Lee, M. J. Piao, S.-J. Jeon and B. R. Cho, *Chem. Mater.*, 2004, ***16***, 2783.

65 H.-Y. Ahn, K. E. Fairfull-Smith, B. J. Morrow, V. Lussini, B. Kim, M. V. Bondar, S. E. Bottle and K. D. Belfield, *J. Am. Chem. Soc.*, 2012, ***134***, 4721.

66 The two-photon absorption cross section of a BODIPY similar to **4**, but lacking the two iodine substituents, is only 4 GM at 800 nm (D. Zhang, Y. Wang, Y. Xiao, S. Qian, X. Qian, *Tetrahedron* **2009**, *65*, 8099). This modest value suggests that the presence of the anthracene donor is essential to capture effectively the exciting near-infrared photons.

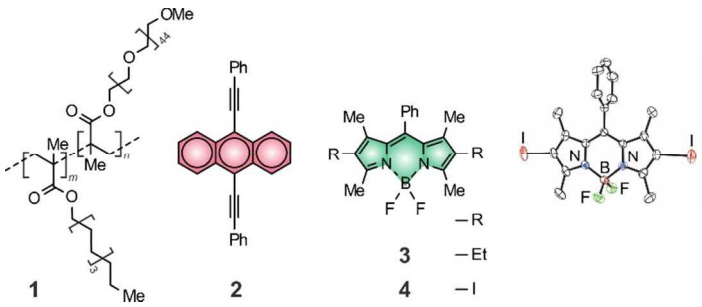

Fig. 1. Structures of amphiphilic polymer **1**, energy donor **2**, energy acceptors **3** and **4** together with ORTEP representation (40% thermal ellipsoid probability) of the geometry of **4** in single crystals.

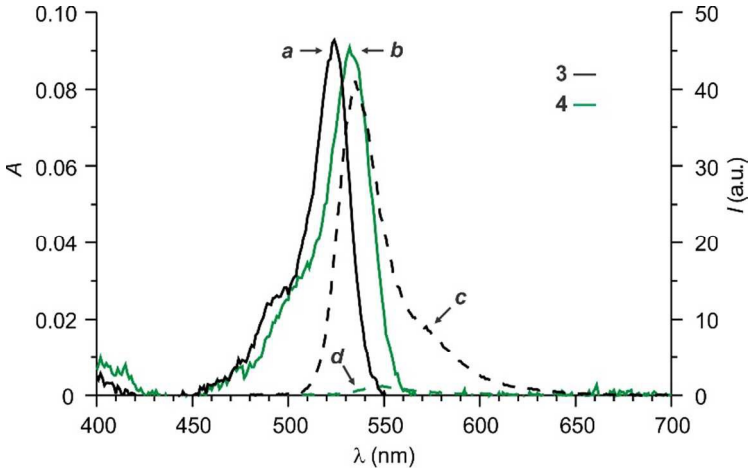

Fig. 2. Absorption (***a*** and ***b***) and emission (***c*** and ***d***, λ_{Ex} = 470 nm) spectra of THF solutions (1.0 μM, 25 °C) of **3** and **4**.

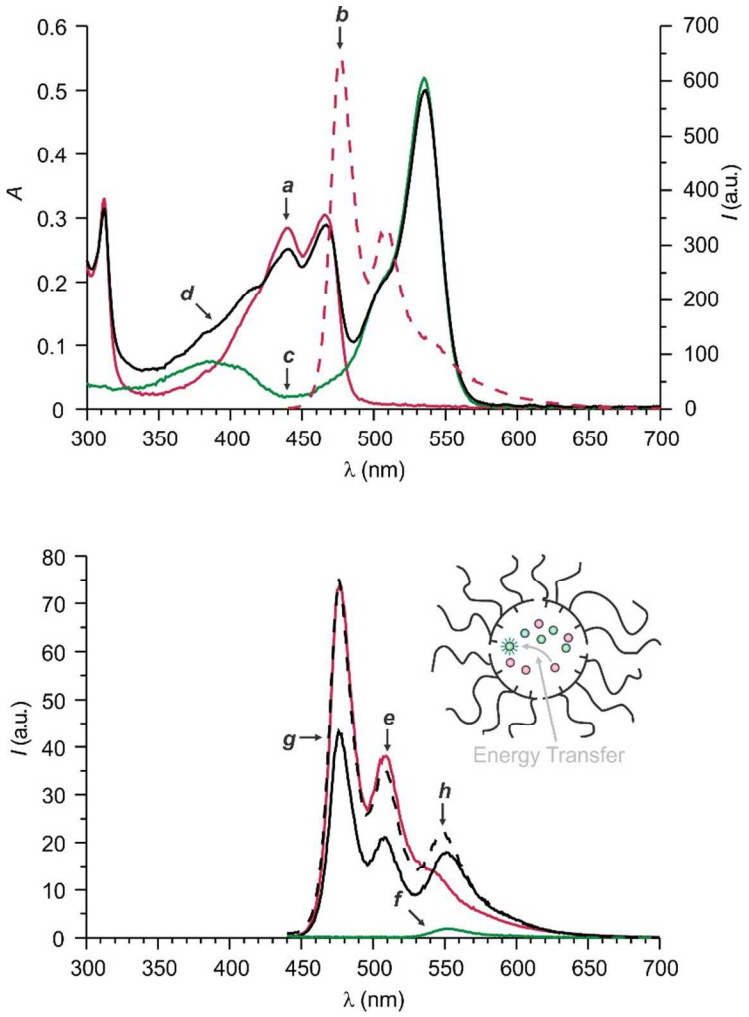

Fig. 3. Absorption (***a***, ***c*** and ***d***) and emission (***b*** and ***e***–***h***, λ_{Ex} = 430 nm) spectra of PBS solutions (pH = 7.0, 25 °C) of nanoparticles of **1** (500 μg mL^{-1}), containing **2** (***a***, ***b*** and ***e***, 5 μg mL^{-1}), **4** (***c*** and ***f***, 5 μg mL^{-1}) or both compounds (***d*** and ***g***, 5 μg mL^{-1} each). Emission spectrum (***h***) recorded, under the same conditions, after mixing a PBS solution (pH = 7.0, 25 °C) of nanoparticles of **1** (500 μg mL^{-1}), containing **2** (10 μg mL^{-1}), with an equal volume of a PBS solution (pH = 7.0, 25 °C) of nanoparticles of **1** (500 μg mL^{-1}), containing **4** (10 μg mL^{-1}). Spectrum ***e*** is normalized to ***h***.

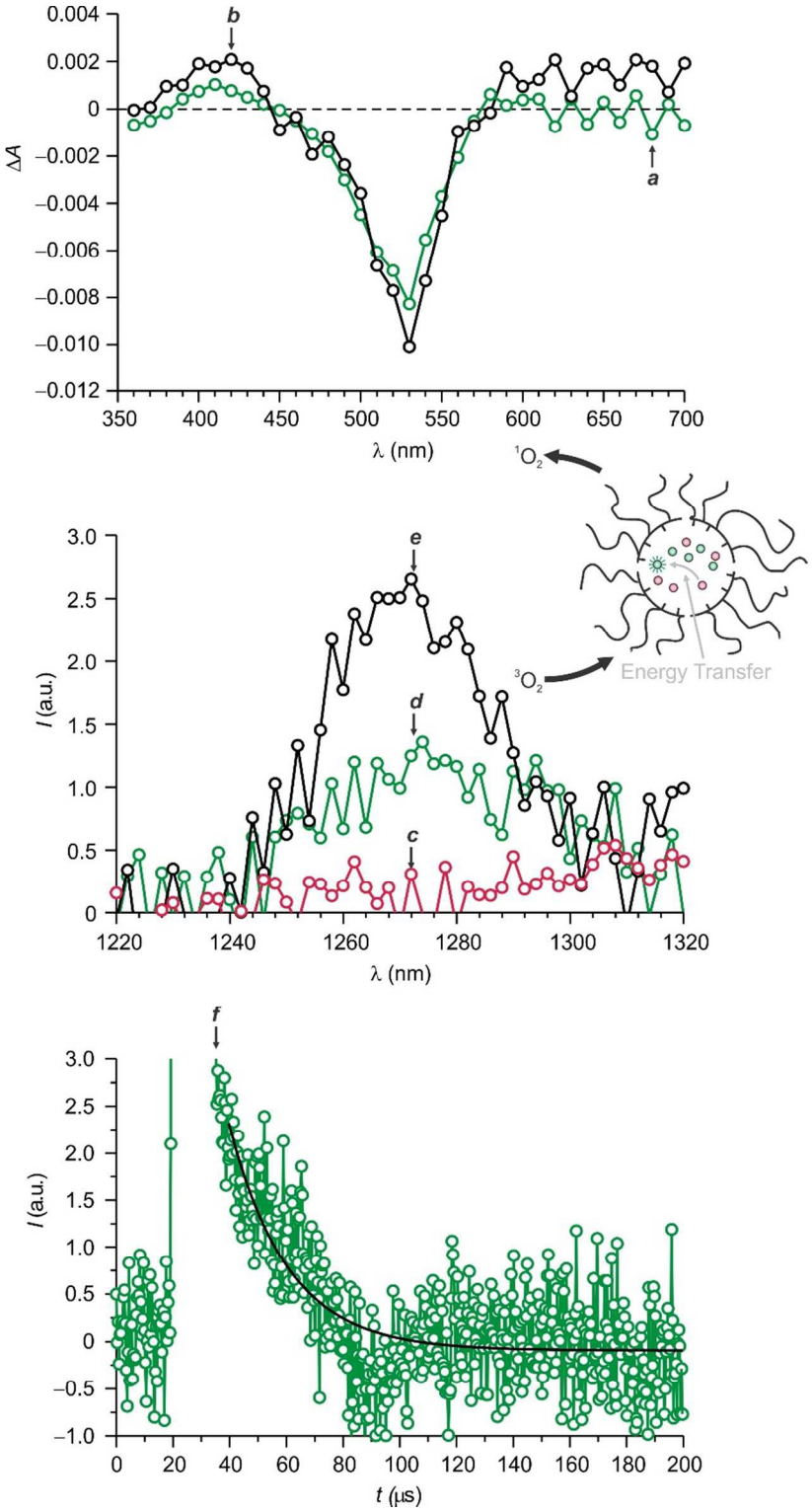

Fig. 4. Transient absorption spectra, recorded 0.1 μs after pulsed-laser excitation (355 nm, 6 ns, 12 mJ per pulse), of degassed PBS solutions (pH = 7.0, 25 °C) of nanoparticles of **1** (500 μg mL^{-1}), containing **4** (0.2 μg mL^{-1}) without (***a***) and with (***b***) **2** (1.2 μg mL^{-1}). Emission spectra (λ_{Ex} = 405 nm)

of aerated deuterated PBS solutions (pH = 7.0, 25 °C) of nanoparticles of **1** (500 μg mL^{-1}), containing **2** (***c***, 1.2 μg mL^{-1}), **4** (***d***, 0.2 μg mL^{-1}) or both compounds (***e***). Evolution of the emission intensity (***f***) at 1270 nm of an aerated deuterated PBS solution (pH = 7.0, 25 °C) of nanoparticles of **1** (500 μg mL^{-1}), containing **4** (0.2 μg mL^{-1}), upon pulsed-laser excitation (355 nm, 6 ns, 12 mJ per pulse).

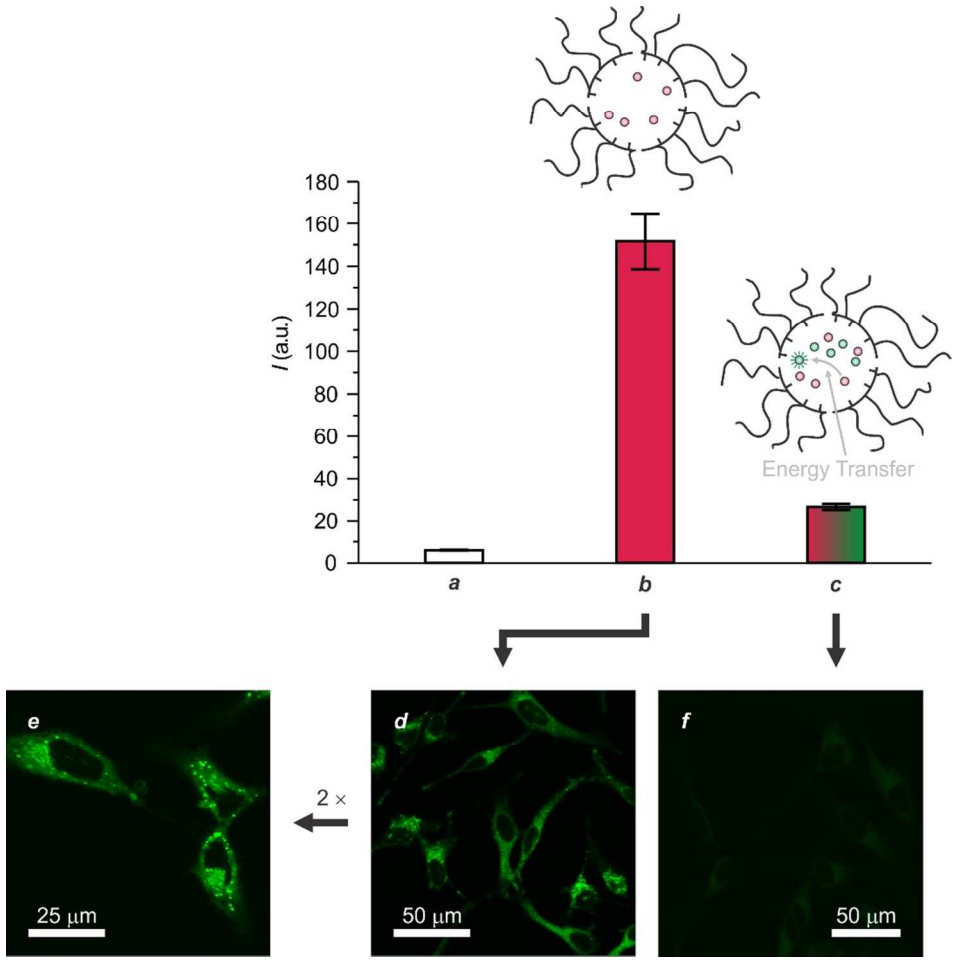

Fig. 5. Emission intensities (λ_{Ex} = 435 nm, λ_{Em} = 470 nm) recorded with a plate reader before (***a***) and after, as well as fluorescence images (λ_{Ex} = 459 nm, λ_{Em} = 470–520 nm) recorded after, incubation of HeLa cells with either (***b***, ***d*** and ***e***) a PBS solution (50 μL) of nanoparticles of **1** (125 μg mL^{-1}), containing **2** (2.5 μg mL^{-1}) and PBS (50 μL), or (***c*** and ***f***) a PBS solution (50 μL) of nanoparticles of **1** (125 μg mL^{-1}), containing **2** (2.5 μg mL^{-1}), and a PBS solution (50 μL) of nanoparticles of **1** (125 μg mL^{-1}), containing **4** (2.5 μg mL^{-1}), for 3 hours and washing.

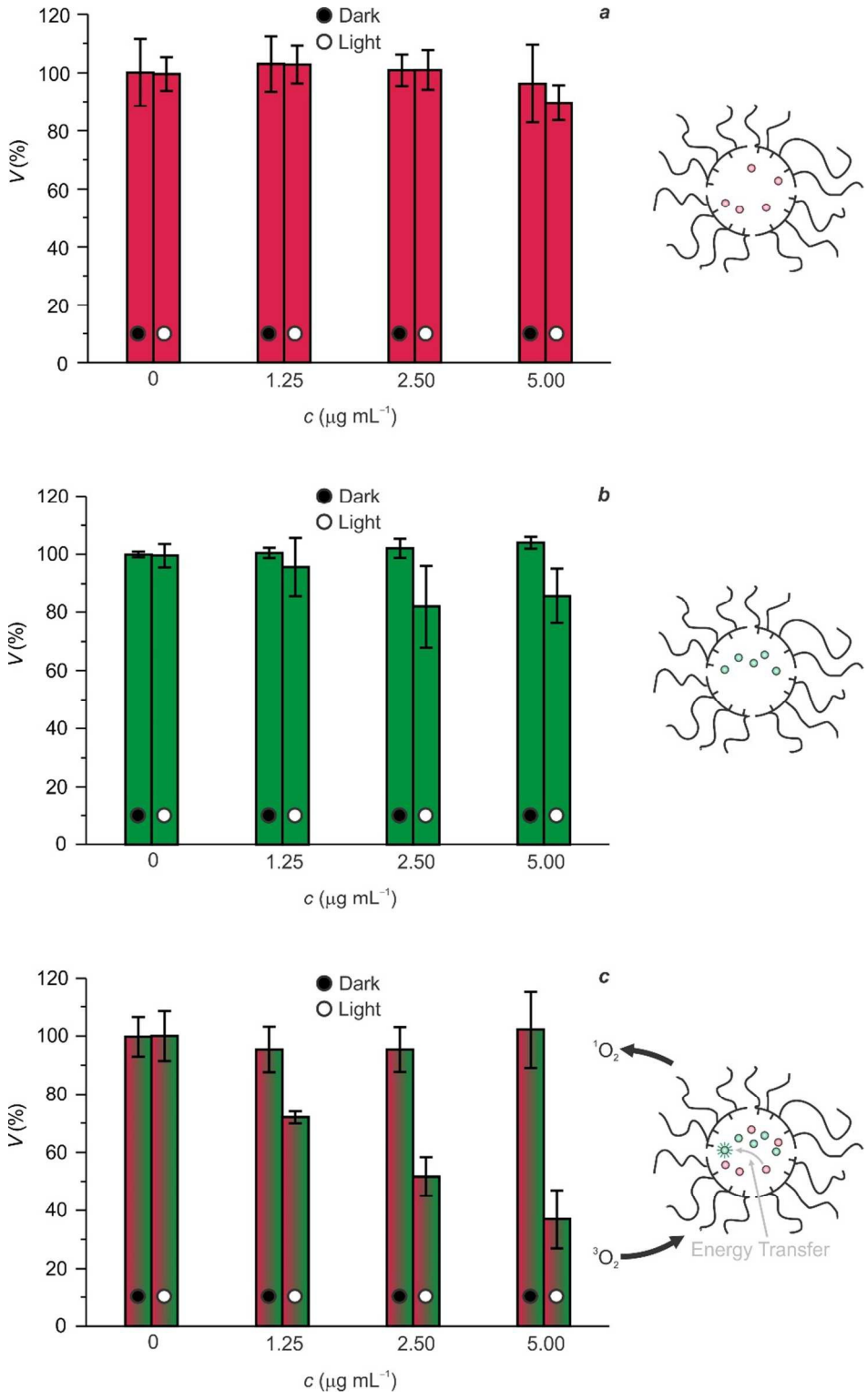

Fig. 6. Viability of HeLA cells recorded after incubation with PBS solutions of nanoparticles of **1** (125 μg mL^{-1}), containing increasing amounts of either **2** (***a***) or **4** (***b***), or with mixtures (1:1, v/v) of the two

solutions (***c***) for 3 hours, washing and either storage in the dark for 24 hours or irradiation with a continuous-wave laser (435 nm, 5 mW) for 30 s and subsequent storage in the dark for 24 hours.

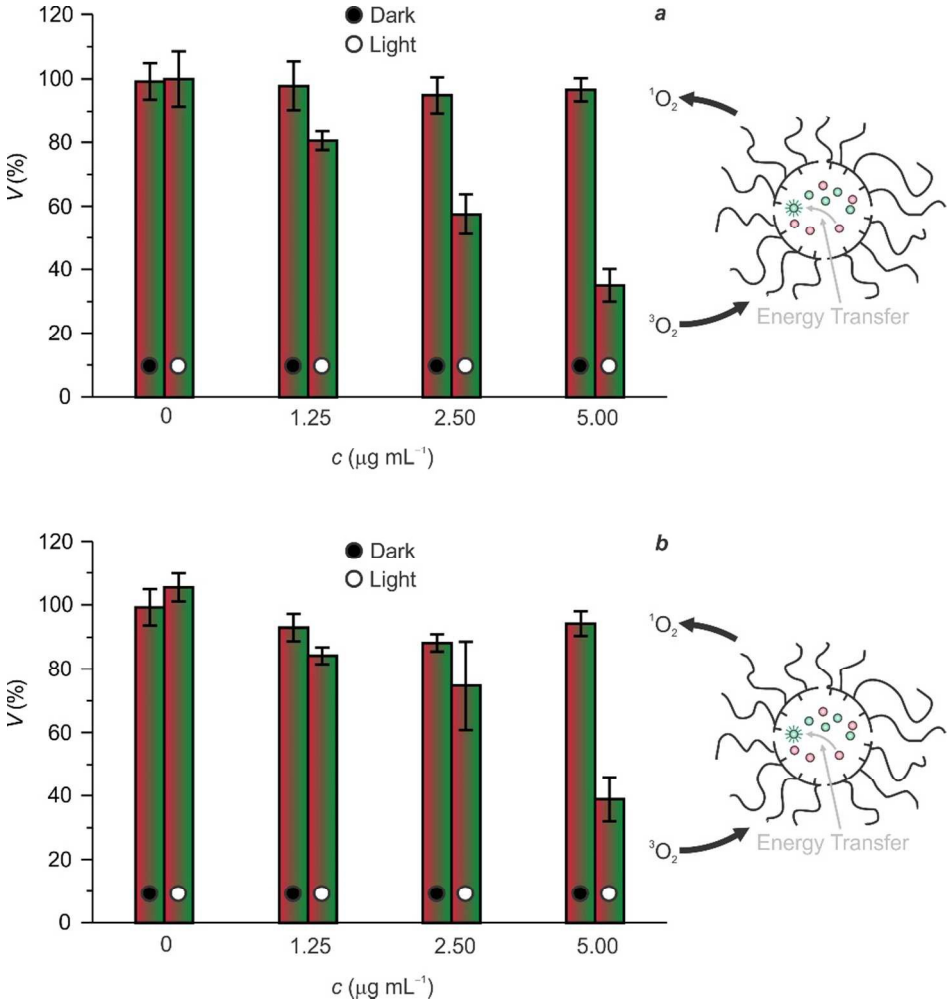

Fig. 7. Viability of HeLA cells recorded after incubation with PBS solutions of nanoparticles of **1** (125 μg mL^{-1}), containing increasing amounts of either **2** (***a***) or **4** (***b***), for 3 hours, washing and incubation with PBS solutions of nanoparticles of **1** (125 μg mL^{-1}), containing equivalent amounts of either **4** or **2** respectively, washing and either storage in the dark for 24 hours or irradiation with a continuous-wave laser (435 nm, 5 mW) for 30 s and subsequent storage in the dark for 24 hours.

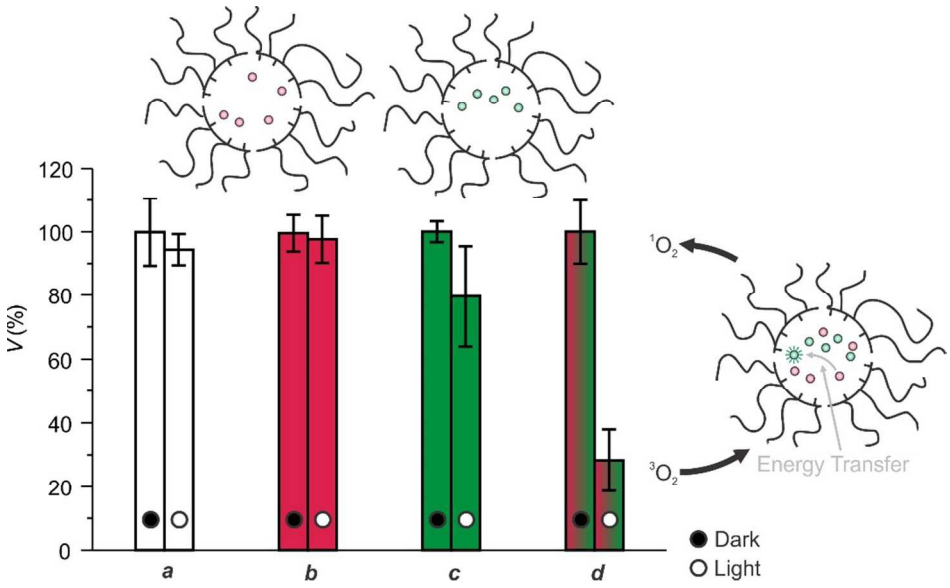

Fig. 8. Viability of HeLA cells recorded before (***a***) and after incubation with a PBS solution of nanoparticles of **1** (125 μg mL^{-1}), containing either **2** (***b***, 2.5 μg mL^{-1}) or **4** (***c***, 2.5 μg mL^{-1}), or with a mixture (1:1, v/v) of the two solutions (***d***) for 3 hours, washing and either storage in the dark or irradiation with a pulsed laser (100 fs, 900 nm, 80 mW) for 30 s and subsequent storage in the dark for 24 hours.

Graphical Abstract

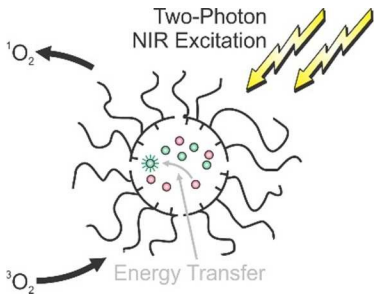

Supramolecular nanocarriers, co-entrapping complementary donors and acceptors within their hydrophobic interior, enable the intracellular generation of singlet oxygen upon near-infrared excitation